EDOCROS: EARLY DETECTION OF CROP WATER AND NUTRITIONAL STRESS BY REMOTELY SENSED INDICATORS

C. Panigada (1), L. Busetto (1), M. Meroni (1,2), S. Amaducci (3), M. Rossini (1), S. Cogliati (1), M. Boschetti (4), V. Picchi (5), A. Marchesi (6), F. Pinto (7), U. Rascher (7), R. Colombo (1)

(1) DISAT-LTDA, Department of Environmental Sciences, Remote Sensing of Environmental Dynamics Laboratory, University of Milano-Bicocca, Milano, Italy
*Piazza della Scienza 1, 20126 Milan, Italy, Email: **cinzia.panigada@unimib.it**, lorenzo.busetto@unimib.it, michele.meroni@unimib.it, micol.rossini@unimib.it, s.cogliati3@campus.unimib.it, andrea.marchesi@unimib.it, roberto.colombo@unimib.it*
(2) Joint Research Center (JRC)- Ispra VA, Italy
(3) Università cattolica di Piacenza, Piacenza, Italy, Email: stefano.amaducci@unicatt.it
(4) CNR-IREA, Via Bassini 15, Milano, Italy, Email: boschetti.m@irea.cnr.it
(5) National Council for Agricultural Research, CRA, Research Unit for Agri-Food Processes, via G. Venezian 26 20133 Milano, Italy, Email: valentina.picchi@entecra.it
(6) Building Environment Sciences and Technology Department (BEST) -,Politecnico di Milano University , Piazza Leonardo da Vinci 32, 20133 Milano Italy, Email: andrea.marchesi@polimi.it
(7) Institut für Chemie und Dynamik der Geosphäre, ICG-3: Phytosphäre, Forschungszentrum Jülich GmbH, 52425 Jülich, Email: f.pinto@fz-juelich.de, u.rascher@fz-juelich.de

ABSTRACT

In the framework of ESA Fluorescence campaigns 2010, the EDOCROS (Early Detection Of CROp Stress) campaign, supported by EUFAR (European Facility For Airborne Research project) was aimed to detect early crop stress due to water and nitrogen (N) deficit, by means of advanced hyperspectral remote sensing techniques.

CASI 1500 (Itres, Canada), AISA eagle (Specim, Finland) and AHS-160 (Sensytech Inc., USA) imagery were acquired contemporary to an intensive field campaign where vegetation biophysical and eco-physiological measurements were collected. Canopy spectral measurements were also acquired on corn parcels with different N and water treatments by means of a PS and a SWIR Spectral Camera (Specim, Finland) mounted on a cherry picker with a nadir view.

In this paper the EDOCROS campaign is presented with particular focus on field data acquisition and analysis. Furthermore, preliminary results of analysis conducted on AISA eagle imagery are presented and discussed. Different vegetation indices were calculated, and relative values of sun-induced chlorophyll fluorescence at 760 nm (F_{760}) were retrieved by the FLD (Frahunofer Line depth) method [1]. The regression analysis between hyperspectral data and field parameters showed that red edge indices combined with soil adjusted indices (TCI/OSAVI and MTCI/MSAVI) were highly correlated with leaf relative chlorophyll content (SPAD values), minimizing the effect of canopy structure (Leaf Area Index – LAI) and soil background. F_{760} was highly correlated with canopy relative chlorophyll content (LAI*SPAD), while PRI was highly correlated to light use efficiency measured at leaf level.

1. INTRODUCTION

Hyperspectral remote sensing techniques allow the early detection of vegetation stress, before the appearance of visible symptoms. The most promising of these techniques are represented by the passive measurement of sun-induced fluorescence (Fs) [1], and by the analysis of the Photochemical Reflectance Index (PRI), related to de-epoxidation cycle of xanthophylls and to heat dissipation [2]. These early detection indicators related to plant physiological processes (i.e. light use efficiency), together with narrowband indices related to biophysical parameters (i.e. chlorophyll content and Leaf Area Index, LAI) allow a real time monitoring of the crop status at landscape level. Remote observations in the thermal domain have also been often used for water stress detection since the stomatal conductance decrease related to water stress may cause an increase in canopy temperature [3]. The objective of the EDOCROS experiment was to test the suitability of hyperspectral data (Vegetation Indices - VIs, PRI and Fs) and thermal measurements at field and landscape scale for precision farming applications focused on the early detection of water and nitrogen deficit.

Field radiometric measurements and airborne imagery allowed to test different stress detection techniques at field canopy level and landscape level. Vegetation biophysical parameters (e.g. LAI, fraction of absorbed photosynthetically active radiation fAPAR, leaf pigment relative content, leaf water content) and eco-physiological parameters (e.g. stomatal conductance, fluorescence of chlorophyll a, leaf PRI) were measured in field during the airborne survey to provide a description of crop status and to provide data necessary to parameterize the models used to characterize the stress status from aerial data and to validate their accuracy. Preliminary results are presented and discussed.

2. MATERIALS AND METHODS

2.1. Experimental design and Field Data Collection

Experimental design: the experiment consisted in a split-plot design with four blocks. In each block three water regimes (rainfed, water deficit imposed between stem elongation and flowering and full irrigation,, Irr0, Irr1 and Irr2, respectively) were randomly assigned, while two crop species (corn and sorghum) and two fertilization levels (0 and 100 kg/ha N, N0 and N1, respectively) were assigned to split plots (subplots defined by water regime). Parcel size was 15 m * 16.5 m with a total study area of about 2 ha centred at latitude 44° 58.820' N and longitude 9° 40.817' E. The experimental scheme is depicted in Fig. 1. The seedling was conducted on May the 3rd 2010 and the field campaign was held between July the 19th and the 22nd 2010.

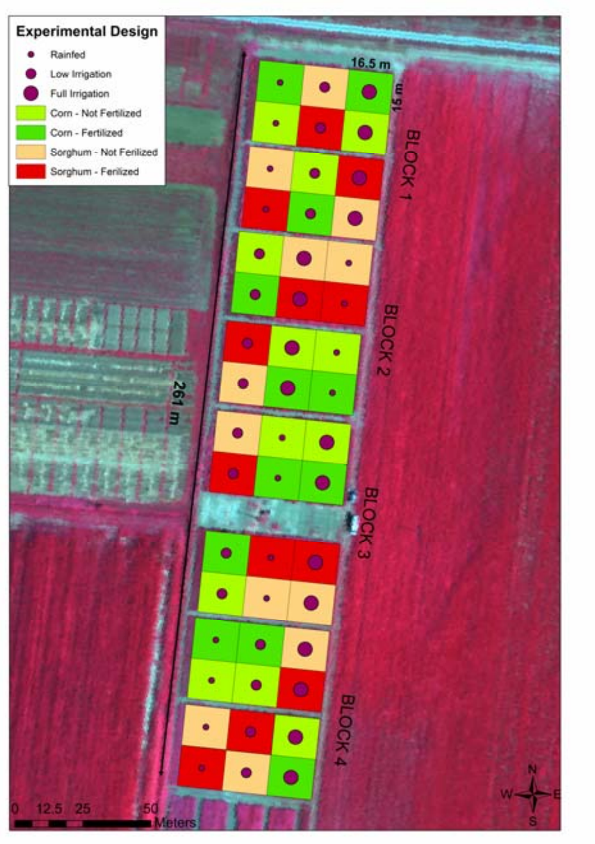

Figure 1. Experimental design.

Leaf level measurements: Table 1 summarizes the leaf level measurements collected during the field campaign.

Table 1. Leaf level parameters collected in field. Relative chlorophyll was collected with a SPAD 502 meter (Minolta, Japan), PRI with a PlantPen (PSI, Czech Republic), fluorescence parameters ΔF/Fm' and Fv/Fm with a MiniPAM (Walz, Germany), gas exchange parameters, i.e. instantaneous assimilation (Ai), stomatal conductance to water vapour (Gi), intercellular CO_2 concentration (Ci) and transpiration rate (Ti) with a CIRAS-1 (PP-Systems, UK), field and laboratory light curves and A/Ci curves with a Licor-6400 XT (LI-COR Biosciences, USA).

Parameter	Species	Plants	Parcels	Blocks
Relative Chl	corn/sorghum	10	48	4
PRI	corn/sorghum	10	48	4
ΔF/Fm'	Corn	15	24	4
Fv/Fm	Corn	15	24	4
Ai	Corn	3	6	1
Ci	Corn	3	6	1
Gi	Corn	3	6	1
Ti	Corn	3	6	1
Lab light curves	Corn	3	12	2
A/Ci	Corn	2	12	2
Field light curves	Corn	2	6	1

Leaf relative chlorophyll content, leaf PRI, active fluorescence of chlorophyll *a* parameters and gas exchange parameters were measured in corn and sorghum parcels between July the 19th and the 20th. Measurements were conducted on the youngest fully expanded leaf. The measurements were repeated around 8.30, 11.30 and 14.30 UTC, contemporary to the airborne overpasses, except for the relative chlorophyll content which does not show a day trend and was therefore measured only at 11:30.
Leaf samples were also collected in all corn parcels in order to extract foliar pigments (i.e. carotenoids and total chlorophyll). Additional samples were collected in corn N1 parcels in order to calculate the leaf equivalent water thickness (EWT) and the relative water content (RWC).
In this paper only preliminary results on corn data are reported.

Canopy level measurements: canopy parameters such as plant density, plant height, and biomass were measured in each parcel. Leaf area index and fAPAR were computed from measurements conducted with a Delta-T SunScan System. Hemispherical photos acquired from ground level with a Nikon Cool Pix 4500digital camera equipped with a fish-eye lens (Nikon FE-E8 8mm) were also used for LAI computation.
Both the SunScan measurements and the hemispherical photos were acquired along a transect crossing two consecutive crop rows at approximate the parcel centre. For each parcel, 10 Suncan measurements and 5 photos were acquired.
Meteo data: Air temperature, relative humidity, precipitation and wind speed were continuously recorded by an automatic meteorological station.

Spectroradiometric measurements: Canopy reflectance was acquired with an hyperspectral sensor mounted on a cherry picker. Images were acquired from about 6 m height (investigated area of about 2 m^2) on 6 corn parcels characterized by different water and N treatments (two fully irrigated fertilized parcels and two not fertilized, one rainfed fertilized parcel and one not fertilized). Three images were acquired for each parcel. Furthermore, images were acquired on a single parcel every 30 minutes from 10.40 to 16.10 in order to investigate the daily trend of passive fluorescence and narrowband VIs.

Ancillary data: spectroradiometric measurements of white and black panels located close to the experimental field and of different natural targets (e.g. soil, asphalt) were collected by an ASD Fieldspec PRO radiometer during the airborne survey for calibration and validation of atmospheric corrections. Sunphotometer measurements were acquired to provide atmospheric optical thickness data for atmospheric correction. Finally, ground control points were acquired by a high precision differential global positioning system Trimble Geo-XT in order to support the geometric correction of remotely sensed data and to allow the precise identification of field sampling points on the aerial imagery.

2.2. Remotely sensed imagery and pre-processing

An airborne campaign was conducted by the Spanish Instituto Nacional de Técnica Aerospacial (INTA) on July the 19^{th}. Images were acquired with a CASI 1500 (Itres, Canada) and an AHS-160 (Sensytech Inc., USA) sensor. Three surveys were scheduled at 8.30, 11.30 and 14.30 UTC in order to highlight photoprotection, fluorescence and temperature differences related to plant water stress during the course of the day. A second survey was conducted on July the 20^{th} at 12:30 UTC by the Italian Istitito Nazionale di Oceanografia e Geofisica Sperimentale (OGS), using an AISA eagle hyperspectral sensor (Specim, Finland). In tables 2 and 3 the sensor and the acquired imagery characteristics are presented.

In this paper only preliminary results on AISA eagle data are reported.

The AISA eagle image was georeferenced and atmospherically corrected by an empirical line approach. Five ground reflectance spectra measured in field on different targets (white and black panels, two soils and asphalt) identified in the image were used.

Table 2. Sensor characteristics and spectral region covered; FWHM is the full width at half maximum; FOV is the instantaneous field of view.

Sensor	Spectral Range nm)	N° of bands	FWHM (nm)	IFOV (mrad)
AISA	394-968	244	2.3	0.5
CASI 1500	380–1050	72	2.4 – 14.4	0.5
AHS	430-1030	20	28	2.5
	1550-1750	1	200	
	2000-2560	42	13	
	3300-5400	7	300	
	8200-12700	10	400	

Table 3. Sun-sensor configuration in the different runs acquired during the overflights; acquisition time is reported in UTC; θ_s is the solar zenith angle.

RUN	Time (UTC)	θ_s (°)	Heading (referred to solar plane)
CASI #1	08:40	42	Principal
CASI #2	08:49	41	Perpendicular (*)
CASI #3	08:58	40	Perpendicular (**)
CASI #4	11:24	24	Principal
CASI #5	14:20	43	Principal
AHS #1	08:26	45	Principal
AHS #2	11:04	25	Principal
AHS#3	14:01	40	Principal
AISA #1	12:37	29	Principal

** Experimental field observed in the hot spot*
*** Experimental field observed in the dark spot*

2.3. Computation of vegetation indices and fluorescence

Mean reflectance values were extracted from a 3x3 pixel area (9 m^2) located on AISA eagle image in correspondence of the center of each of the 24 corn parcels. Several narrowband optical indices were calculated from mean reflectance (table 4).

Table 4. Summary of narrowband optical indices analysed in this work. R_X is the reflectance at the specified wavelength x in nanometers. F_{760} is the extracted fluorescence signal by FLD method.

Index	Formulation	Reference
NDVI	$(R_{800}-R_{680})/(R_{800}+R_{680})$	[4]
OSAVI	$(1+0.16)*(R_{800}-R_{670})/(R_{800}+R_{670}+0.16)$	[5]
NDI	$(R_{750}-R_{705})/(R_{750}+R_{705})$	[6]
VOG	R_{740}/R_{720}	[7]
REP	λ at R maximum derivative in the range (690-740nm)	[8]
TCARI	$3*[(R_{700}-R_{670})-0.2*(R_{700}-R_{550})*(R_{700}/R_{670})$	[9]
TCARI/ OSAVI	TCARI/OSAVI	[10]
TCI	$[1.2*(R_{700}-R_{550})-1.5*(R_{670}-R_{550})*(R_{70}0/R_{670})^{0.5}]$	[10]
TCI/ OSAVI	TCI/OSAVI	[10]
MTCI	$(R_{753.75}-R_{705})/(R_{705}-R_{681.25})$	[11]
MTCI/ MSAVI	$MTCI/[0.5*(2*R_{800}+1-((2*R_{800}+1)^2-8*(R_{800}-R_{670})^2)^{0.5}]$	[10]
PRI	$(R_{531}-R_{570})/ (R_{531}+R_{570})$	[2]
SIPI	$(R_{800}-R_{445})/(R_{800}-R_{680})$	[12]
PSRI	$(R_{680}-R_{500})/R_{750}$	[13]
F_{760}	FLD method	[1]

These indices were chosen because they are representative of different categories related to green biomass, chlorophyll content and light use efficiency. NDVI is the most known and widely used vegetation index related to LAI. The optimized soil adjusted vegetation index (OSAVI) is part of the family of soil adjusted VIs (SAVI) which compensate for soil background influences. Its determination does not need information on soil optical properties and it showed the best overall performance for most agricultural crops [5]. The normalized difference index (NDI), the red edge position (REP), the MERIS terrestrial chlorophyll index (MTCI) and the simple ratio VOG are indices related to the reflectance changes in the red edge, which are related to chlorophyll content but also influenced by LAI. The transformed chlorophyll absorption index (TCARI) and the triangular chlorophyll index (TCI) measure the depth of chlorophyll absorption and have shown fairly good correlation with leaf chlorophyll concentration if combined with soil adjusted vegetation indices (i.e. TCARI/OSAVI, TCI/OSAVI) [9, 10]. The combined index MTCI/MSAVI was also tested. The plant senescence reflectance index (PSRI) and the structure insensitive pigment index (SIPI) related to foliar pigment composition (i.e., carotenoid and chlorophyll ratio (car/chl)), were also investigated to monitor plant stress. Finally, PRI was computed as well known early stress detection indicator correlated to plant light use efficiency.

AISA eagle at sensor radiances (FWHM = 4.2 nm at 760 nm and a spectral sampling of 2.43 nm, independently estimated with SpecCal, [14]) were also used to estimate fluorescence at the O_2-A band (F_{760}) using the standard FLD approach [1]. Fluorescence emerging from top of the canopy (TOC) was computed according to the method proposed by [15] which requires the presence of non fluorescent targets in the scene to compute the atmospheric transmittance and path radiance inside and outside the absorption feature. A set of non fluorescent image targets represented by white and black panels, soils and asphalt were used to estimate the two constants (k_1 and k_2) required for the computation of the relative fluorescence values (i.e., k_3*F_{760}, hereafter only called F_{760}) as shown in equation 1:

$$k_3*F_{760} = L_{in} - k_1 * L_{out} + k_2 \qquad \text{[Eq. 1]}$$

Poor results were achieved using one single band in the absorption feature. The resulting fluorescence image was noisy and showing some evident artefacts (i.e., striping) probably due to low signal to noise ratio of the selected spectral channel. A better image quality was achieved at the expenses of a reduction of the spectral resolution, that is, using two channels inside the absorption band (centred at 761.037 and 763.4 nm) and two outside (centred at 753.7 and 756.1 nm).

2.4. Statistical analysis

Field data (i.e. SPAD, LAI, gas analyzer parameters, chlorophyll fluorescence parameters and leaf PRI) were analysed by general linear models (GLM) followed by the Least Significance Difference (LSD) test to test for the effects of irrigation level, N treatment and the interaction between different treatments. All mentioned analyses were performed with the software package Statistica 6.0 (StatSoft Inc., Tulsa, USA).

Relationships between field data and remotely extracted data (VIs and F_{760}) were evaluated by ordinary least squares (OLS) regression analysis. In order to compare the regression accuracy the determination coefficients (R^2) were computed and the significance of regressions was tested.

3. RESULTS AND DISCUSSION

3.1. Field data analysis

Structural, biochemical and physiological parameter mean values are reported in table 5 and table 6 for N0 and N1, respectively. Their variability depends on the stress imposed (i.e. N and water treatment), even though differences were not always significant.

Results of the statistical analysis (reported by letters in table 5 and 6) showed that water availability affects corn by increasing mean LAI and relative chlorophyll content (SPAD values) in both fertilization treatments, even though differences are not always significant. This is confirmed by the higher photosynthetic performances evidenced in irrigated (Irr2) parcels by instantaneous assimilation (Ai), fluorescence yield (ΔF/Fm') and leaf PRI values. Irr 1 N0 parcels show low PRI values but high ΔF/Fm' and Ai values. Since PRI is inversely related to carotenoids and total chlorophyll ratio (car/chl) [16], low PRI values may be related to an increase in the carotenoid pool experienced by plants grown in chronic water stress deficiency.

EWT calculated only in fertilized samples does not show any significant difference, while RWC shows lower values in Irr0 and Irr1 than in Irr2.

For what concern the fertilization (statistical analysis results not reported) it is shown that fertilization increased the level of LAI and SPAD values only in irrigated parcels (Irr1 and Irr2). This suggests that water availability was the limiting factor in the experiment. Differences were instead evidenced in photosynthetic performances as shown by Ai, ΔF/Fm' and leaf PRI that increased in fertilized parcels.

Table 5. Field parameter values in corn not fertilized parcels (N0). Values represent means ± standard deviations calculated for each water treatment (Irr0, Irr1, Irr2). Different letters indicate statistically different values at p = 0.05.

Parameter	N 0		
	Irr 0	Irr 1	Irr 2
LAI	2.11± 0.92 a	2.02± 0.85 a	2.68± 0.07 a
SPAD	49.6± 5.2 a	47.2± 5.8 b	50.3± 5.2 a
PRI (*10^3)	1.49± 7.32 b	2.74± 7.81 b	7.15± 7.15 a
ΔF/Fm'	0.309± 0.077 b	0.369± 0.048 a	0.386± 0.054 a
Ai	30.83± 3.01 b	39.28± 3.89 a	40.01± 4.11 a

Table 6. Field parameter values in corn fertilized parcels (N1). Values represent means ± standard deviations calculated for each water treatment (Irr0, Irr1, Irr2). Different letters indicate statistically different values at p = 0.05.

Parameter	N 1		
	Irr 0	Irr 1	Irr 2
LAI	1.98± 0.54 b	2.66± 0.22 ab	3.16± 0.64 a
SPAD	50.1± 4.1 c	52.5± 3.8 b	55.2± 3.8 a
RWC	0.93± 0.03 b	0.92± 0.02 b	0.95± 0.02 a
EWT	0.0127± 0.0011 a	0.0130± 0.0008 a	0.0134± 0.0009 a
PRI (*10^3)	9.23± 8.88 b	7.71± 8.40 b	13.9± 6.57 a
ΔF/Fm'	0.345± 0.071 b	0.351± 0.070 b	0.396± 0.065 a
Ai	33.17± 2.67 b	34.45± 4.43 b	44.85± 3.91 a

3.2. Remotely sensed data analysis

The different narrowband indices were tested in order to identify best relationships with structural, biochemical and physiological corn parameters sensible to water and N stress. Results of the regression analysis between field data, i.e. LAI, SPAD, ΔF/Fm' and VIs calculated from AISA eagle image are reported in Table 7. Best fittings were always obtained with linear models. SPAD values were multiplied by LAI (i.e. LAI*SPAD) to provide a proxy of canopy chlorophyll content.

Best correlations with LAI were obtained by red edge simple ratio indices (NDI R^2 = 0.72, VOG R^2 = 0.69) that showed higher performances than NDVI (R^2 = 0.62).

Indices measuring the depth of chlorophyll absorption (TCI, TCARI) showed a weak correlation with SPAD values. The performances improved considerably when these indices were combined with OSAVI confirming previous finding by [10]. TCI/OSAVI and TCARI/OSAVI increased the correlation with SPAD (R^2 = 0.53 and R^2 = 0.64, respectively), in particular the TCI/OSAVI showed higher ability in responding to SPAD variations, minimizing LAI and soil background effects. Similar behaviour was observed in MTCI which improved significantly its correlation with SPAD when combined with MSAVI (MTCI R^2 = 0.49, MTCI/MSAVI R^2 = 0.65).

PRI showed a good correlation with LAI (R^2 = 0.65), and moderate correlation with ΔF/Fm' (R^2 = 0.49), while no correlation was found with SPAD values. Stressed plants showed low LAI values and low PRI values that means high car/chl ratio (typical of photo-oxidative stress symptoms). This was also evidenced by SIPI and PSRI indices. Further investigations are needed (e.g. total chlorophyll and carotenoid extraction and quantification) to confirm this result.

F_{760} was correlated with LAI (R^2 = 0.58) while moderately correlated with SPAD values (R^2 = 0.31). Correlation increased significantly with LAI*SPAD (R^2 = 0.66). Moderate correlation was found with ΔF/Fm' (R^2 = 0.36). An attempt to minimize LAI and background effect was conducted by combining F_{760} with MSAVI and OSAVI indices, but the correlation with ΔF/Fm' did not increase.

*Table 7. Correlations between vegetation indices calculated from AISA eagle image and corn biophysical and physiological variables (SPAD, LAI, SPAD *LAI and ΔF/Fm'). R^2 is the determination coefficient which indicates the accuracy of the fitting. All the regressions are significant at p = 0.05.*

VI	R^2			
	LAI	SPAD	LAI* SPAD	ΔF/Fm'
NDVI	0.62	n.s.	0.53	0.39
OSAVI	0.69	n.s.	0.60	0.48
NDI	0.72	n.s.	0.69	0.50
VOG	0.69	n.s.	0.71	0.52
REP	0.21	0.32	0.30	n.s.
TCARI	n.s.	0.43	n.s.	n.s.
TCARI/OSAVI	0.19	0.64	0.34	n.s.
TCI	0.22	0.20	n.s	n.s.
TCI/OSAVI	n.s.	0.53	n.s.	n.s.
MTCI	0.52	0.49	0.67	0.37
MTCI/MSAVI	0.22	0.65	0.39	0.18
PRI	0.65	n.s.	0.62	0.49
SIPI	0.62	n.s.	0.54	0.45
PSRI	0.65	n.s.	0.55	0.44
F_{760}	0.58	0.31	0.66	0.36

4. CONCLUSIONS

In this study we showed preliminary results of the EDOCROS project, aimed at testing the suitability of airborne RS data for detecting water and nutritional stress in corn under different levels of fertilization (0 and 100 kg/ha) and irrigation (rainfed, full irrigation and water deficit imposed in critical phenological phases). Field data collected during the airborne campaign were analysed. We observed that structural, biochemical and physiological parameters showed variability as function of the stress status at the time of the flight overpass. Different narrowband indices were calculated and sun-induced fluorescence signal F_{760} was extracted using the FLD method. Red edge indices combined with soil adjusted indices (TCI/OSAVI and MTCI/MSAVI) showed the best correlation with relative chlorophyll values, confirming their ability in minimizing LAI and soil background effect. PRI was highly correlated with ΔF/Fm' while no correlation was found with SPAD values. We can hypothesize that an increase in the carotenoid pool is experienced in water stressed crops without a decrease in chlorophyll content. Finally F_{760} was correlated to relative canopy chlorophyll content.

Further development of this research will focus on the analysis of CASI 1500 data acquired during the EDOCROS campaign including the exploitation of different methods for retrieving the fluorescence signal. The complete set of images (multi-angular and multi-temporal overpasses) will also improve the understanding of the influence of canopy structure, background and viewing geometry on remotely-sensed PRI and F_{760}. Furthermore, thermal data not presented in this paper will be also investigated with the aim to develop a combined optical and thermal crop stress index.

ACKNOWLEDGMENTS

This research was funded by Axìa (CRUI-Nestlé project for research and development). Flights were conducted in the frame of EUFAR (European Facility For Airborne Research project) Transnational Access project. The authors gratefully acknowledge C. Cilia, T. Julitta, B. Di Mauro, M. Ferretti (DISAT-UNIMIB, Italy), M. Bergonti (Università Cattolica di Piacenza).

REFERENCES

1. Meroni, M., M. Rossini, L. Guanter, et al., 2009, Remote sensing of solar-induced chlorophyll fluorescence: Review of methods and applications, Remote Sens. Environ., **113**(10): p. 2037-2051.
2. Gamon, J.A., J. Penuelas, and C.B. Field, 1992, A narrow-waveband spectral index that tracks diurnal changes in photosynthetic efficiency, Remote Sens. Environ., **41**(1): p. 35-44.
3. Suarez, L., P.J. Zarco-Tejada, G. Sepulcre-Canto, et al., 2008, Assessing canopy PRI for water stress detection with diurnal airborne imagery, Remote Sens. Environ., **112**(2): p. 560-575.
4. Rouse, J.W., R.H. Haas, J.A. Schell, et al., *Monitoring the Vernal Advancements and Retro Gradation of Natural Vegetation*, in *NASA/GSFC Final Report* 1974: Greenbelt, MD, USA. p. 371.
5. Rondeaux, G., M. Steven, and F. Baret, 1996, Optimization of soil-adjusted vegetation indices, Remote Sens. Environ., **55**(2): p. 95-107.
6. Gitelson, A.A. and M.N. Merzlyak, 1996, Signature analysis of leaf reflectance spectra: Algorithm development for remote sensing of chlorophyll, Journal of Plant Physiology, **148**(3-4): p. 494-500.
7. Vogelmann, J.E., B.N. Rock, and D.M. Moss, 1993, Red Edge Spectral Measurements from Sugar Maple Leaves, International Journal of Remote Sensing, **14**(8): p. 1563-1575.

8. Curran, P.J., W.R. Windham, and H.L. Gholz, 1995, Exploring the Relationship between Reflectance Red Edge and Chlorophyll Concentration in Slash Pine Leaves, Tree Physiology, **15**(3): p. 203-206.
9. Haboudane, D., J.R. Miller, N. Tremblay, et al., 2002, Integrated narrow-band vegetation indices for prediction of crop chlorophyll content for application to precision agriculture, Remote Sens. Environ., **81**(2-3): p. 416-426.
10. Haboudane, D., N. Tremblay, J.R. Miller, et al., 2008, Remote estimation of crop chlorophyll content using spectral indices derived from hyperspectral data, IEEE Trans. Geosci. Remote Sensing, **46**(2): p. 423-437.
11. Dash, J. and P.J. Curran, 2004, The MERIS terrestrial chlorophyll index, International Journal of Remote Sensing, **25**(23): p. 5403-5413.
12. Penuelas, J., F. Baret, and I. Filella, 1995, Semiempirical Indexes to Assess Carotenoids Chlorophyll-a Ratio from Leaf Spectral Reflectance, Photosynthetica, **31**(2): p. 221-230.
13. Merzlyak, M.N., A.A. Gitelson, O.B. Chivkunova, et al., 1999, Non-destructive optical detection of pigment changes during leaf senescence and fruit ripening, Physiologia Plantarum, **106**(1): p. 135-141.
14. Meroni, M., L. Busetto, L. Guanter, et al., Characterization of fine resolution field spectrometers using solar Fraunhofer lines and atmospheric absorption features, Applied Optics, **49**(15): p. 2858-2871.
15. Maier, S.W., K.P. Günther, and M. Stellmes. *Remote sensing and modelling of solar induced fluorescence*. in *1st Workshop on Remote Sensing of Solar Induced Vegetation Fluorescence*. 2002. ESTEC, Noordwijk, The Netherlands.
16. Stylinski, C.D., J.A. Gamon, and W.C. Oechel, 2002, Seasonal patterns of reflectance indices, carotenoid pigments and photosynthesis of evergreen chaparral species, Oecologia, **131**(3): p. 366-374; Panigada, C., M. Rossini, M. Meroni, et al., 2009, Indicators of ozone effects on Fagus sylvatica L. by means of spectroradiometric measurements, Rivista Italiana Di Telerilevamento, **41**(2): p. 3-20.
17. Zarco-Tejada, P.J., J.A.J. Berni, L. Suarez, et al., 2009, Imaging chlorophyll fluorescence with an airborne narrow-band multispectral camera for vegetation stress detection, Remote Sens. Environ., **113**(6): p. 1262-1275.